GLOBAL BIOGEOCHEMICAL CYCLES, VOL. 9, NO. 4, PAGES 621–636, DECEMBER 1995

Global ocean phosphate and oxygen simulations

Laurence A. Anderson

Division of Applied Sciences, Harvard University, Cambridge, Massachusetts

Jorge L. Sarmiento

Progam in Atmospheric and Oceanic Sciences, Princeton University, Princeton, New Jersey

Abstract. We examine the role of dissolved organic matter (DOM) and the stoichiometric ratios of organic matter remineralization in determining the magnitude and distribution of remineralization of organic matter in the oceanic water column, and the impact of this remineralization on tracer distributions. Our aim is to improve the parameterization of relevant processes in ocean general circulation models by bringing the models into closer agreement with new observational constraints that suggest substantial differences from previous work (lower DOM levels and higher $-O_2/P$ ratios). We used phosphate and apparent oxygen utlilization (AOU) to analyze the effect of the remineralization profile on water column tracer distributions. The primary impact of DOM cycling is to modify the distribution of remineralization over that obtained from a model with particle cycling only. Changing the oxygen-to-phosphorus stoichiometric ratio modifies the magnitude of oxygen utilization, but preserves its basic distribution. We find that even a small amount of DOM is sufficient to prevent the problem of nutrient trapping. Improved phosphate and AOU simulations are obtained when the amount of DOM is reduced and the deep ocean $-O_2/P$ ratio is increased in accord with recent observations of these properties.

1. Introduction

The cycling of carbon by oceanic organisms plays a major role in determining the partitioning of CO_2 between the atmosphere and ocean as well as the spatial distribution of air-sea CO_2 fluxes. The dominant role of CO_2 as a greenhouse gas is the major motivation behind the development of models of the ocean biosphere aimed at understanding its behavior. The processes that must be simulated in such models include the formation of organic carbon in the surface by uptake of inorganic carbon, the transport of organic carbon from the surface to the abyss, and remineralization of the organic matter at depth. A first generation of three-dimensional model simulations of these processes demonstrated their feasibility and the usefulness of such models in improving our understanding of nutrient and carbon cycling in the oceans. The first models had simple parameterizations of biological production as well as remineralization. A second generation of studies is now beginning to include more sophisticated process models and to examine the sensitivity of the models to various ways of parameterizing those processes.

The study described here is an attempt by us to examine what is perhaps the least understood of the relevant biological processes, namely, the remineralization of organic matter at depth. We begin with the *Najjar et al.* [1992] simulations of the phosphate distribution as a basis. These models simulated the production of organic matter in the surface by the simple expedient of forcing the model predicted phosphate content toward observations. Such an approach guarantees that the surface phosphate will be close to observed. The nutrient removed during a given time step is converted to organic matter.

Paper number 95GB01902.
0886-6236/95/95GB-01902$10.00

An early version of these models was developed before the suggestion that dissolved organic matter might play a major role in export from the surface. The production of organic matter was placed entirely into particles that were remineralized in the water column immediately below where they were produced according to a power law vertical structure determined from sediment trap observations. This simulation gave large anomalies, the most notable of which was exceptionally high nutrients at thermocline depths below regions of high upwelling. This "nutrient trapping" was found to be dramatically reduced when, in response to new evidence that dissolved organic matter could play a dominant role in transport from the surface [*Suzuki et al.*, 1985; *Sugimura and Suzuki*, 1988], *Najjar* [1990] and *Najjar et al.* [1992] put 80% of the export production into dissolved organic matter and only 20% into particles [cf. also *Bacastow and Maier-Reimer*, 1991]. The dissolved organic matter could move laterally away from the upwelling regions before being remineralized, and thus avoid the trapping of nutrients beneath these regions.

An additional major problem with the *Najjar et al.* [1992] particle-only simulation was that the phosphate concentration was lower than observed in the main thermocline and higher than observed at depth. Invoking dissolved organic matter cycling also helped to diminish this discrepancy. It did so by increasing the remineralization in the main thermocline. An alternative approach that also helped with this particular problem was to use an exponential particle remineralization profile with a long length scale, rather than the power law scaling based on sediment trap observations.

New observational studies since the *Najjar et al.* [1992] simulations raise a number of questions about the use of dissolved organic matter to improve model simulations. The high concentrations of dissolved organic nitrogen and carbon that were observed by *Suzuki et al.* [1985] and *Sugimura and Suzuki* [1988] turned

out to be erroneous [*Suzuki*, 1993]. New observations give much lower dissolved organic concentrations in general, and suggest that the the labile part of the dissolved organic matter pool is found in relatively shallow waters. Furthermore, observations of dissolved organic phosphorus [e.g., *Ridal and Moore*, 1990] suggest that the ratio of this tracer to dissolved organic nitrogen and carbon is well below the stoichiometric ratios of *Redfield et al.* [1963], contrary to the assumption that had been made by *Najjar et al.* [1992].

A first aim of this study was to reexamine the issues that had been raised by the *Najjar et al.* [1992] simulation in the light of the new measurements of dissolved organic matter. We show here that it does not take a large amount of dissolved organic phosphorus to avoid nutrient trapping beneath upwelling regions. However, if the dissolved organic phosphorus concentration is reduced, the problem of too low phosphate concentrations in the main thermocline reappears. We argue here that the most likely explanation for this anomaly is that the model thermocline physics is incorrect, a hypothesis that had been proposed by *Najjar et al.* [1992] but which they did not pursue any further. We show additional evidence here supporting this view.

The second major aim of this study was to build on the work of *Najjar* [1990] to demonstrate the power of apparent oxygen utilization (AOU) as a tracer of organic matter remineralization in the water column, and to examine important issues relating to this tracer. Since most of the oxygen utilization is by oxidation of organic carbon, we argue that AOU observations provide an excellent test of a model's capacity to model the carbon cycle. *Najjar* [1990] found that he could obtain a good fit to AOU observations with an $-O_2/P$ ratio of 138:1. A considerable amount of empirical work suggests that a more appropriate ratio is 170±10 [*Takahashi et al.*, 1985; *Broecker et al.*, 1985; *Anderson and Sarmiento*, 1994]. The use of this higher $-O_2/P$ ratio in his models gave *Najjar* [1990] considerably worse simulations. We demonstrate here that a ratio of 170 gives a far better fit to observations once the phosphate simulation is modified as above.

A third and final aim was to examine the sensitivity of the AOU simulation to the $-O_2/P$ ratio in waters shallower than 400 m, where the ratio is not so well constrained and there are some who argue that it may be different from 170. For example, *You and Tomczak* [1993] suggest an $-O_2/P$ ratio of 135 for the upper ocean. By contrast, *Sambrotto et al.* [1993] suggest a C_{org}/N uptake ratio of roughly 10 at the ocean surface; assuming an N/P ratio of 16 and an $-O_2/C_{org}$ ratio of 1.4, this suggests an $-O_2/P$ ratio of $10 \times 16 \times 1.4 = 224$. We investigate the problem by allowing the upper ocean $-O_2/P$ ratio to vary. We find that a value of 170 gives a better upper ocean AOU distribution than 138, but that the deep ocean AOU distribution is not highly sensitive to the ratio chosen. In agreement with this, E. Maier-Reimer (personal communication, 1995) has used model results from a simulation with a constant Redfield ratio to demonstrate that the result of *You and Tomczak* [1993] may be an artifact of their analysis technique.

2. Model Description

The physical model used in this study is that of *Najjar et al.* [1992], which is also the "prognostic" global ocean general circulation model of *Toggweiler et al.* [1989a, b]. As this model has been extensively discussed previously, only a brief summary will be given here. The model is of the world ocean, with 4.5° latitude by 3.75° longitude resolution, 12 vertical levels to 5000 m, and realistic bathymetry. Motion is governed by the primitive equations under the Boussinesq, rigid lid, and hydrostatic approximations, with potential temperature and salinity being used as dynamically active tracers. The surface ocean is forced by annual *Hellerman and Rosenstein* [1983] wind stresses, and heat and freshwater fluxes determined by relaxing the surface layer temperature and salinity to *Levitus* [1982] annual observations.

The biological component of the model is essentially identical to simulation S4 of *Najjar et al.* [1992]. Phosphate, dissolved organic phosphorus, and oxygen are passive tracers that are advected and diffused by the physical circulation, and affected by the oceanic biological cycle as described below. Justifications for the following parameterizations are given by *Najjar* [1990] and *Najjar et al.* [1992].

New production is determined by restoring phosphate in the euphotic zone to observations whenever surface phosphate exceeds observations, that is,

$$\text{new production} = (1/\tau)([PO_4] - [PO_4]^*) \qquad \text{if } [PO_4] > [PO_4]^*$$

$$\text{new production} = 0 \qquad \text{otherwise}$$

The euphotic zone is defined as levels 1 and 2 of the model, which extend to a depth of 119.3 m. Here $[PO_4]^*$ is the observed phosphate concentration and τ is a restoring time constant.

A certain fraction (σ) of new production is used to generate dissolved organic phosphorus (DOP), while the remainder ($1 - \sigma$) is put into particulate organic phosphorus (POP). POP is immediately transferred out of the euphotic zone, such that the flux of POP at the base of the euphotic zone at any particular location is

$$F_e = (1 - \sigma) \int_{-z_e}^{0} (\text{new production})\ dz$$

Here z_e is the depth of the euphotic zone (z being depth, that is, positive and increasing in magnitude downward). The vertical flux of POP beneath the euphotic zone is parameterized following the POC observations of *Martin et al.* [1987], as

$$F(z) = F_e\,(z / z_e)^{-0.858}$$

Remineralization occurs immediately and is equal to $-dF(z)/dz$. All POP reaching the deepest ocean box at any given location is immediately remineralized in that box.

DOP is allowed to advect and diffuse out of the euphotic zone, and once below the euphotic zone it remineralizes at a rate proportional to its concentration

$$\text{DOP remineralization rate} = \kappa\,[\text{DOP}]$$

where κ is in units of s^{-1}, such that $1/\kappa$ can be thought of as the effective timescale of DOP remineralization, or DOP lifetime. Here κ is parameterized as decreasing exponentially with depth to reflect the fact that water column bacterial abundance decreases with depth [*Cho and Azam*, 1988], namely,

$$\kappa = \kappa' \exp((z_e - z) / 750)$$

Here κ' is a constant factor determined by the model such that the production and remineralization of DOP balance, that is,

$$\kappa' = \sigma \int_A \int_{-z_e}^{0} (\text{new production})\ dz\ dA$$

$$/ \int_A \int_{-z_b}^{-z_e} [\text{DOP}] \exp(z_e - z) / 750\ dz\ dA$$

where z_b is the depth of the seafloor at each location. The value of κ is thus dependent on the inventory of DOP in the model.

DOP was not allowed to remineralize in the euphotic zone, so that these experiments could be directly compared with those of *Najjar* [1990] and *Najjar et al.* [1992]. Najjar's original motivation for doing this was so that "production" in the model would be equivalent to new production. Although all of the DOP parameterizations are being reconsidered in our ongoing modeling work (R. Murnane, personal communication, 1994), the changes do not affect the main conclusions of this paper.

Both phosphate and DOP are conserved in the model. In accordance with *Najjar et al.* [1992], mean oceanic PO_4 was chosen as 2.10 μmol/kg. As mean oceanic PO_4 is actually 2.13 μmol/kg [*Levitus et al.*, 1993], all PO_4 "observations" presented in this article have been scaled down by a factor of 2.10/2.13, so that they could be compared with the model results. The choices made for the mean oceanic DOP concentration are discussed in the next section.

The only phosphate model parameters that differ from those of simulation S4 of *Najjar et al.* [1992] are the restoring timescale to surface phosphate conditions (τ), the fraction of new production going into DOP (σ), and the global mean DOP concentration ($[DOP]_{avg}$). Although *Najjar et al.* [1992] used τ = 30 days in their simulations, we have used τ = 100 days. This longer timescale lowers new production in high latitudes to values more in keeping with observation-based estimates (see section 3) and decreases the number of locations where new production is zero [*Najjar*, 1990, pp. 110-118]. This change in τ does not significantly affect the deep ocean phosphate distribution, nutrient trapping, or the denitrification rate [*Najjar*, 1990, pp. 168-170]. This weaker restoring time constant does allow surface phosphate concentrations to be slightly higher than observed; at 25 m depth, phosphate is about 0.05 μmol/kg higher, on average, than when τ = 30 days is used. This is due primarily to increased concentrations at the equator and high latitudes where the upward flux of PO_4 is greatest (see Figure 1). This misfit is within the uncertainty of the phosphate climatology, as well as uncertainty arising from possible errors in the model's physical circulation.

According to *Najjar et al.* [1992, p. 51], observations of oceanic POM fluxes as a fraction of new production suggest values for σ between 0.4 and 0.8. Recent work by *Murray et al.* [1994] in the Equatorial Pacific suggests a value of 0.75. In our simulations we have used σ = 0.5, as a compromise within this range.

Oxygen in the model is removed in the aphotic zone during remineralization as the amount of phophate regenerated (from DOP and POP) times a specified stoichiometric ratio, R_{remin}. If oxygen concentrations reach zero, phosphate remineralization is allowed to occur without oxygen consumption under the presumed circumstances of denitrification. Oxygen is produced in the euphotic zone, as a stoichiometric ratio (R_{photo}) times the amount of phosphate consumed as new production. This euphotic zone ratio is determined by the model so that oxygen production in the euphotic zone balances oxygen consumption in the deep ocean, that is,

$$R_{photo} = \int_A \int_{-z_b}^{-z_e} (\text{oxygen consumption})\ dz\ dA \Big/ \int_A \int_{-z_e}^{0} (\text{new production})\ dz\ dA$$

where new production is in terms of organic phosphorus production. Oxygen consumption is assumed to balance oxygen production because the oxygen "gained" due to the occurrence of denitrification must, in a steady state, be balanced by an oxygen "loss" from nitrogen fixation in the surface ocean. This balance is achieved through the definition of R_{photo}. As such, R_{photo} will differ from the (remineralization-weighted) mean value of R_{remin} if denitrification is occurring. This is always the case in our simulations.

Although the amounts of oxygen produced and consumed by biology balance, oxygen is not conserved in the model ocean at its initial concentration, as it is allowed to exchange freely with

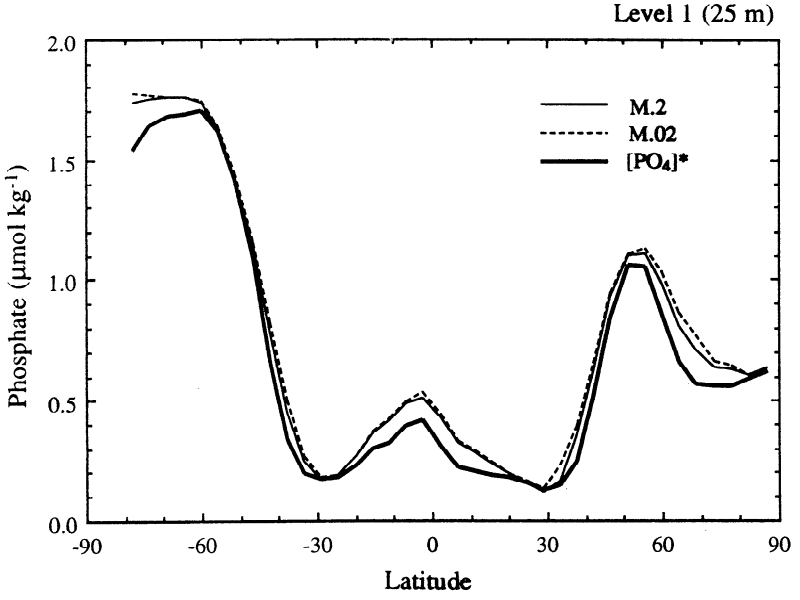

Figure 1. Zonally averaged surface (level 1) phosphate concentrations versus latitude, for models M.2 and M.02, and the field to which the models are restored, $[PO_4]^*$.

the atmosphere, which is treated as an infinite reservoir. Therefore the model ocean's equilibrium oxygen content will vary with different biological scenarios, as a function of the magnitude and pattern of oxygen production at the ocean surface and of oxygen consumption at depth. This allows an examination of how different biological model scenarios affect the oxygen content of the ocean interior.

The flux of oxygen across the sea surface is characterized as

$$F_{O_2} = (1 - f_i)\, k_w\, ([O_2]_{sat} - [O_2])$$

where f_i is the fraction of sea surface area covered by ice, k_w is the piston velocity, and $[O_2]_{sat}$ is the oxygen saturation concentration. Here $[O_2]_{sat}$ is calculated as a function of temperature and salinity from the formula of *Weiss* [1970]. Ice is not included in the model, but its impact on air-sea gas exchange is included through the use of a climatological estimate of f_i based on the data of *Walsh* [1978] and *Zwally et al.* [1983]. The piston velocity k_w, as a function of wind speed u and Schmidt number Sc, was calculated using the *Liss and Merlivat* [1986] equation

$$\begin{aligned} k_w(u, Sc) &= (Sc/600)^{-2/3}\, 0.17\, u && \text{for } u \le 3.6 \text{ m s}^{-1} \\ &= (Sc/600)^{-1/2}\, (2.85\, u - 9.65) && \text{for } 3.6 < u \le 13 \text{ m s}^{-1} \\ &= (Sc/600)^{-1/2}\, (5.9\, u - 49.3) && \text{for } u > 13 \text{ m s}^{-1} \end{aligned}$$

The Liss and Merlivat formulation for k_w was used to keep the model results directly comparable with those of *Najjar* [1990]. *Esbensen and Kushnir* [1981] wind speeds were used for u, and the Sc number was determined using the third-order polynomial fit of *Wanninkhof* [1992] as a function of temperature.

As the physical model had been run previously [e.g., *Toggweiler et al.*, 1989a,b] from which the (approximately) steady state velocity fields were available, the physical model itself was not rerun. Rather, these "frozen" velocity fields and convection statistics as described by *Najjar et al.* [1992] were used with real time diffusion to spin up the biological model from rest. The global ocean was initialized with homogeneous concentrations of PO_4, DOP, and O_2. The model was then run for 2000 years with a time step of 1.2 days. By this time the phosphate, oxygen, and DOP distributions as well as the other biological quantities (e.g., new production, κ, R_{photo}, etc ...) had adjusted to essentially steady state values. Among the phosphate simulations, τ and σ were always kept the same, with only $[DOP]_{avg}$ varied between experiments. In the oxygen equations, only the $-O_2/P$ remineralization ratio (R_{remin}) was varied between experiments.

3. Phosphate Simulations

We now discuss the choice for $[DOP]_{avg}$ used in the model. The straightforward way to estimate the global mean DOP concentration is to base it on direct though scanty DOP observations. DOP measurements give values of ~ 0.15 μmol/L at the ocean surface, decreasing to ≤ 0.01 μmol/L by 500 m [*Ridal and Moore*, 1990]. This would suggest approximately 0.02 μmol/kg as the global mean DOP concentration.

Yet as the role of the phosphorus cycle simulation is to drive the oxygen (and eventually carbon) cycle simulations, the fact needs to be addressed that, had the biological model been based on nitrate cycling rather than phosphate, a much higher level of DOM would be prescribed. The mean amount of "labile" DON in the ocean (i.e., neglecting the well-mixed component, which is presumably refractory) is approximately 3-4 μmol/kg [*Jackson and Williams*, 1985; *Walsh*, 1989; *Benner et al.*, 1992]; when divided by an N/P Redfield ratio of 16, this suggests a DOP level of 0.2 μmol/kg. Similarly, a "labile" DOC component on the order of 20 μmol/kg, divided by a C_{org}/P ratio of 106, would suggest a DOP concentration of 0.2 μmol/kg. That is, the "labile" components of DON and DOC are higher than their proper Redfield proportions to observed DOP by an order of magnitude.

Two phosphate simulations were therefore run, called M.2 and M.02, which used 0.2 μmol/kg and 0.02 μmol/kg, respectively, as values for $[DOP]_{avg}$. They can be thought of as upper and lower limit scenarios. While M.02 might be considered more "realistic" as it is based on actual DOP measurements, M.2 might be more appropriate for driving O_2 simulations, as DOC and DOP appear not to be in Redfield proportions. At even more extreme limits are *Najjar et al.*'s [1992] experiment S4 which uses $[DOP]_{avg}$ = 0.75 μmol/kg (based on *Suzuki et al.*'s [1985] higher DON measurements), and their particle-only model S1 which in effect uses $[DOP]_{avg}$ = 0 μmol/kg.

The globally averaged phosphate profiles simulated by models M.2 and M.02 are shown in Figure 2. It can be seen that the M.2 model-predicted globally averaged phosphate profile is higher than observed below 2000 m, and lower than observed between 400 and 2000 m. Looking at the individual basins (Figure 3), we see that the misfit to observations in the deep ocean is primarily in the Atlantic, with the deep Indian, Pacific, and Southern Ocean concentrations being in fairly good agreement with observations. Conversely, the misfit at intermediate depths occurs in the Indian, Pacific, and Southern Oceans, but not in the Atlantic.

The model's high phosphate values in the deep Atlantic are due to a deficiency in the physical model. In the model, southward North Atlantic Deep Water (NADW) outflow in the Atlantic oc-

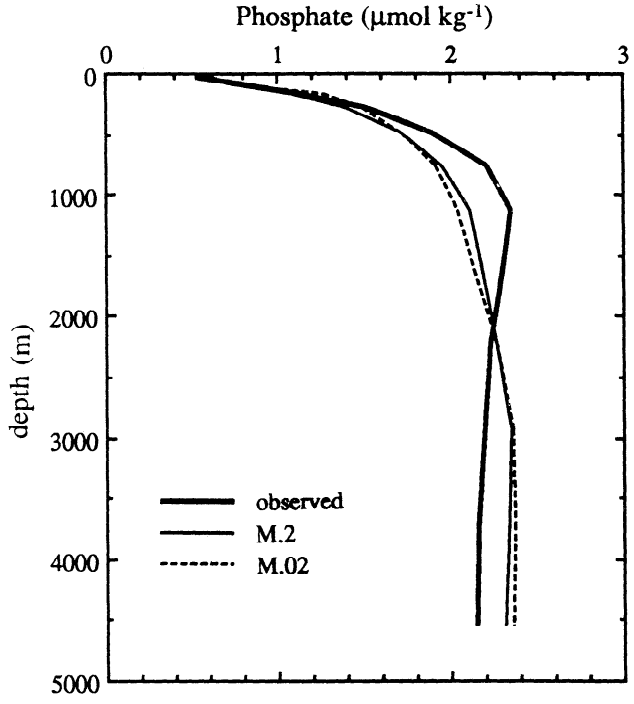

Figure 2. Global mean phosphate concentrations versus depth, as observed and for models M.2 and M.02.

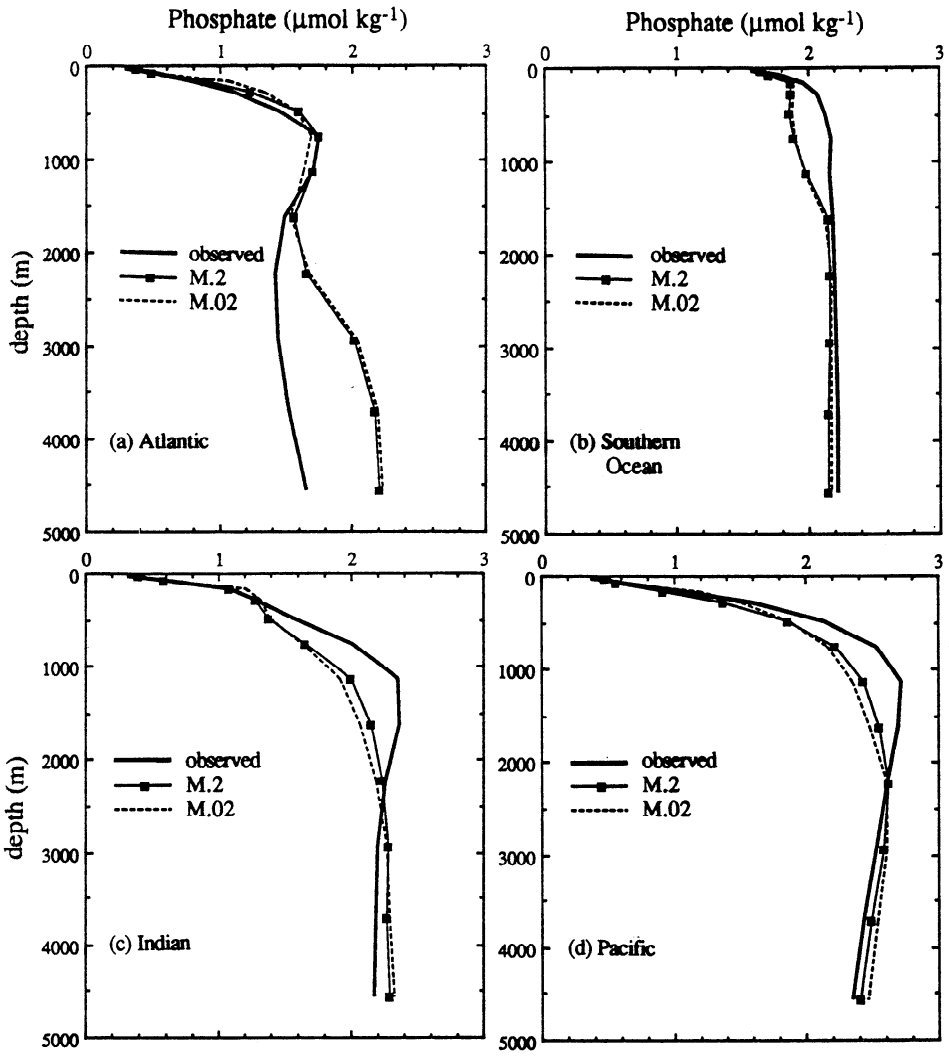

Figure 3. Basin mean phosphate profiles, as observed and for models M.2 and M.02: (a) Atlantic, (b) Southern Ocean (defined as south of 48.9° S), (c) Indian, and (d) Pacific.

curs only between 1347 and 2559 m (i.e., on levels 8 and 9) [*Toggweiler et al.*, 1989a] rather than between approximately 1200 and 4000 meters (levels 8 through 11) as observed [*Bainbridge*, 1981]. As Antarctic Bottom Water (AABW) has a higher preformed phosphate content than NADW, this causes higher-than-observed phosphate concentrations in the deep Atlantic. Figure 4 shows PO_4 versus latitude for all grid boxes on level 11 in the Atlantic for both the model and observations. It can be seen that the model's high average PO_4 value is not the result of excessive remineralization (which would show PO_4 concentrations increasing as AABW flows northward) but rather due to the absence of a low-PO_4 northern end-member as occurs in the observations.

The model's low PO_4 values at intermediate depths may similarly be due to low "preformed" nutrient values. At middepths the model ocean is too warm by up to 4° C (Figure 5a), which suggests that either these levels are ventilated at too low a latitude, or that the vertical mixing rate is too high, allowing more water from lower latitudes into intermediate depths than occurs in reality [*Najjar*, 1990; *Najjar et al.*, 1992]. Either situation would result in the preformed PO_4 values for these depths being too low. In Figure 5b we see that, except in equatorial waters, near-surface phosphate concentrations correlate linearly with potential temperature, such that a thermocline that is too warm by 4° C would be too low in preformed PO_4 by roughly 0.4 μmol/kg. An exception to this is the N. Atlantic, where we see that preformed PO_4 values do not change with temperature, and therefore there would be no such offset. This is generally consistent with what is observed: misfits in the Indian, Pacific, and Southern Ocean thermoclines average 0.3 μmol/kg (the misfit in the Southern Ocean apparently in communication with those of the Indian and Pacific), while there is basically no misfit in the Atlantic. Thus it seems likely that the low PO_4 values at intermediate depths in the model are associated with this "warm thermocline problem" rather than too little biological remineralization.

The vertical PO_4 profiles for model M.02 are also shown in Figures 2 and 3. As can be seen, the M.02 profiles are very similar to those of M.2 for all basins. M.02 phosphate concentrations are slightly lower than those of M.2 at intermediate depths, and slightly higher in the deep ocean, but due to the shortcomings of the physical model it is difficult to say if this means the biological simulation of M.02 is more or less realistic than that of M.2.

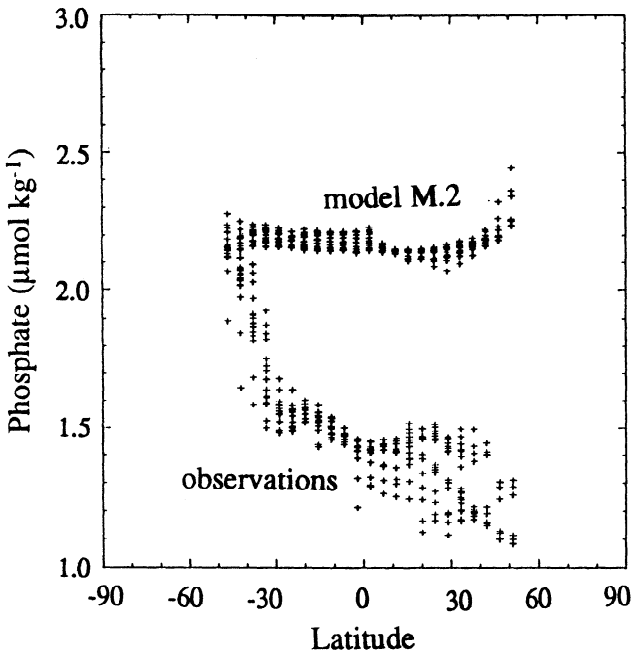

Figure 4. Phosphate versus latitude on level 11 (3721 m depth) in the Atlantic Ocean.

Maps of the phosphate distributions simulated by M.2 and M.02 on model level 4 (295 m) are shown in Figure 6. Both simulations compare favorably with observations, with the M.2 distribution being slightly more realistic than that of M.02. Most importantly, there is no problematic "nutrient trapping" in these models as occurs in the particle-only simulation of *Najjar et al.* [1992], even though M.02 has a very low level of DOP. This is because the main parameter influencing nutrient trapping is not $[DOP]_{avg}$, but σ, the fraction of new production put into DOP versus particles.

New production as a function of latitude is shown in Figure 7. Globally averaged new production in model M.2 (assuming a C_{org}/P ratio of 106) is 2.26 mol C m^{-2} yr^{-1} = 27 g C m^{-2} yr^{-1} = 9.7 Gt C yr^{-1}, and in model M.02 is 2.98 mol C m^{-2} yr^{-1} = 36 g C m^{-2} yr^{-1} = 12.8 Gt C yr^{-1}, which are somewhat higher than estimates based on the vertical flux of particulate organic matter [3-7 Gt C yr^{-1}; *Eppley*, 1989] and lower than estimates from changes in atmospheric oxygen [19 Gt C yr^{-1}; *Keeling and Shertz*, 1992] and ETS activity [22 Gt C yr^{-1}; *Packard et al.*, 1988]. New production in M.02 is 32% higher than in M.2; this is due to the slightly higher phosphate concentrations in M.02 on level 3 (just below the euphotic zone), which is the result of a higher remineralization rate in M.02 on this level, as will be shown. The productivity in the Southern Ocean is not extremely high as it is in Najjar et al.'s model S1 [*Najjar et al.*, 1992, Figure 14], due to the increase of τ to 100 days [*Najjar*, 1990, p. 114]. The low productivities of the subtropical gyres are as expected, but the minima at 60 °S and 50 °N are surprising. Possible causes include an underestimate of the upward flux of PO_4 into the euphotic zone, an overestimate of the observed surface PO_4, or the lack of seasonality in the model. Unfortunately, the actual spatial distribution of annual mean new production is poorly known, so there is little at present with which these calculations can be verified.

The global mean vertical DOP profile for M.02 is shown in Figure 8. Although M.02's mean DOP concentration in the deep ocean is similar to observed (i.e., ≤ 0.01 μmol/kg), in the surface ocean it is much higher than observed (typically ~ 0.15 μmol/kg), with an extremely sharp gradient across the base of the euphotic zone. These high euphotic zone DOP values are required for the vertical transport of new production. In both M.2 and M.02, half of new production goes into DOP (as σ = 0.5); euphotic zone

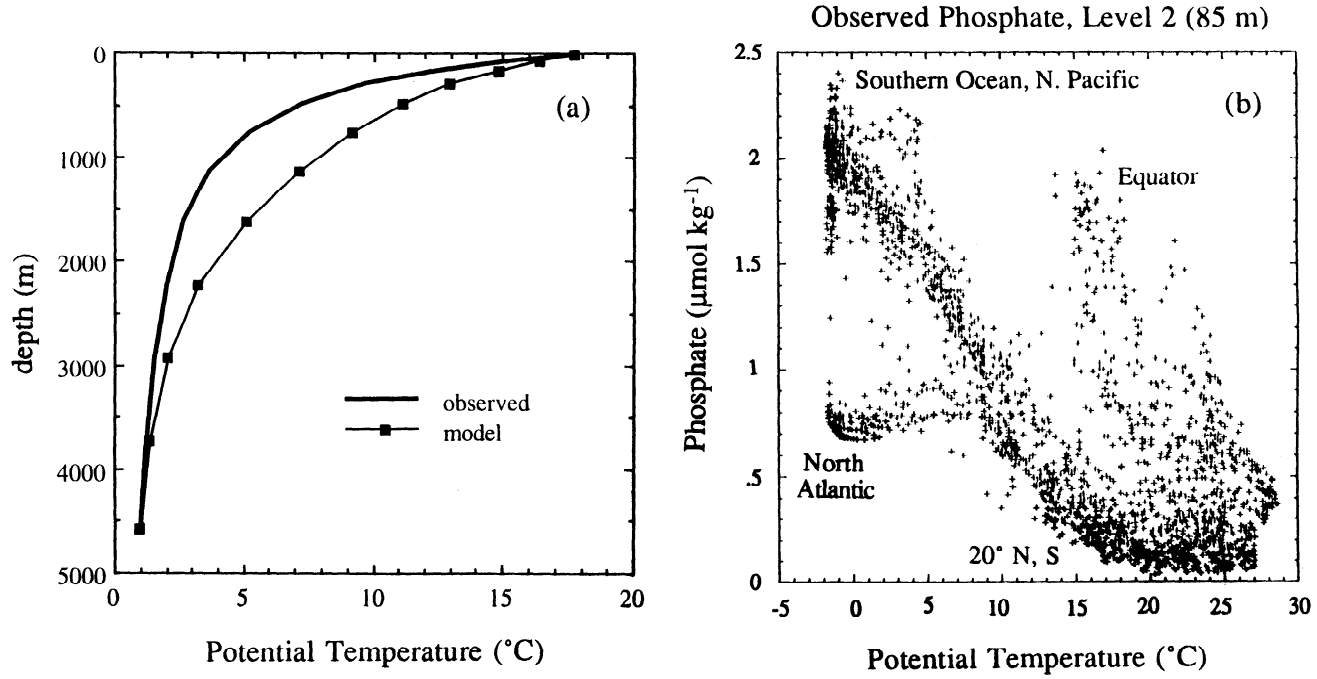

Figure 5. (a) Global mean potential temperature versus depth. (b) Observed phosphate versus potential temperature on level 2 (85 m depth) in the world ocean. Waters with temperatures greater than 15° C are located between 20° N and 20° S, with highest phosphate concentrations occurring at the equator.

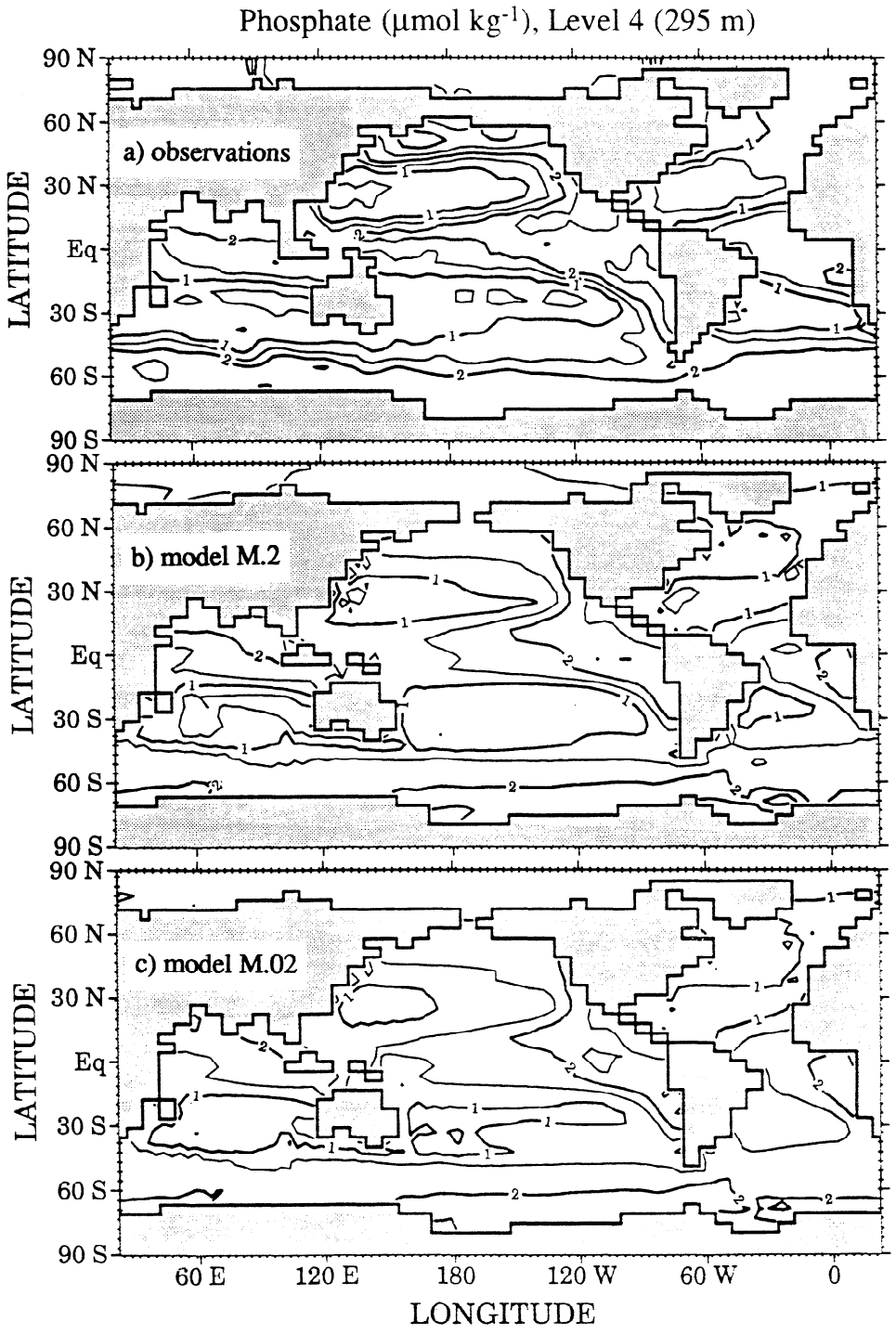

Figure 6. Phosphate at 295 m depth. (a) observations, (b) M.2, (c) M.02. Contour interval = 0.5 μmol/kg.

DOP concentrations and a DOP gradient across the base of the euphotic zone of sufficient sizes are therefore needed so that this production can be exported out of the euphotic zone by advection, convection, and diffusion. As new production is nearly identical in M.2 and M.02, euphotic zone DOP concentrations in M.02 and M.2 are required to be comparable, despite the fact that $[DOP]_{avg}$ in M.02 is an order of magnitude less than in M.2.

The global mean DOP vertical profile as simulated by M.2 is also shown in Figure 8. The values are about an order of magnitude higher than what is actually observed for DOP, although when multiplied by an N/P Redfield ratio of 16 they are comparable to DON observations [*Jackson and Williams,* 1985; *Walsh,* 1989; *Benner et al.,* 1992]. However, the required export of new DOP production in the model causes a large gradient across the base of the euphotic zone that is not well supported by observations.

Values of the quantity $1/\kappa$, which effectively represents DOP lifetime, increase exponentially with depth from 21 years at 170

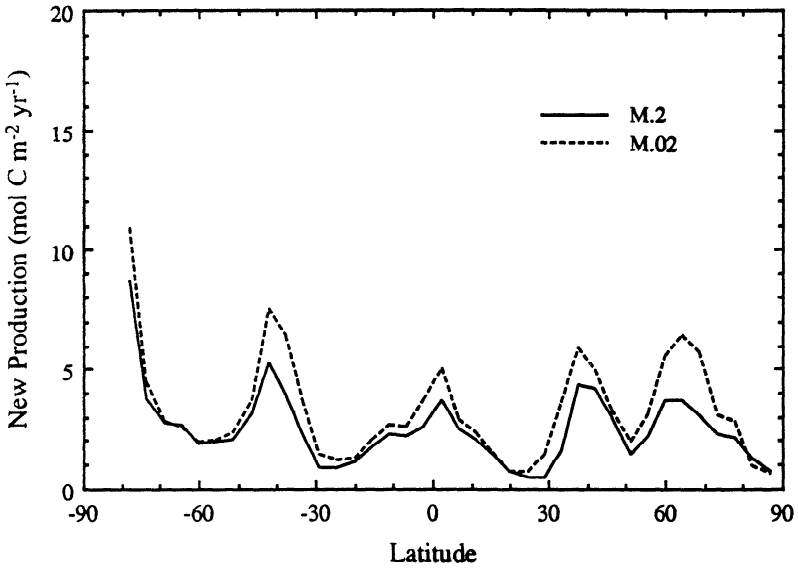

Figure 7. Vertically integrated new production (mol C m^{-2} yr^{-1}) versus latitude, as determined by models M.2 and M.02.

m depth to 7509 years at 4566 m in model M.2, and from 1.1 years to 376 years in model M.02. These deep ocean lifetimes seem rather long for what is being considered "labile" DOM, suggesting that parameterizing the DOP lifetime as an exponential decrease with depth may not be the best approach for modeling DOP.

Horizontally averaged total remineralization rates for M.2 and M.02 are shown in Figure 9. The difference in DOP concentration influences the depth distribution of the remineralization, with M.02 having a shallower remineralization than M.2 above 3000 m. As the production of DOP is nearly the same in both models, the smaller inventory of DOP in M.02 requires a steep decrease in DOP concentration with depth (Figure 8). This is accomplished by a very shallow remineralization. The M.2 simulation has a less steep profile and deeper remineralization. Below 3000 m the remineralization is due primarily to particles, and is higher in M.02 due to its slightly higher new production. Note, however, that despite these differences in the remineralizaton profiles, the phosphate distributions are quite similar (Figure 3). This is because the lower middepth remineralization rates in M.02 are compensated by higher preformed values related to the upper ocean remineralization rates.

In summary, both M.2 and M.02 give reasonably successful phosphate distributions when taking into consideration the limi-

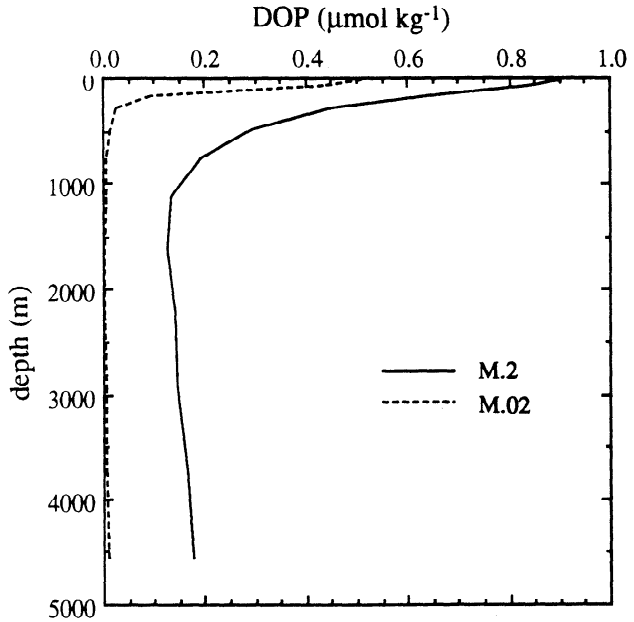

Figure 8. Global mean DOP concentrations versus depth predicted by models M.2 and M.02.

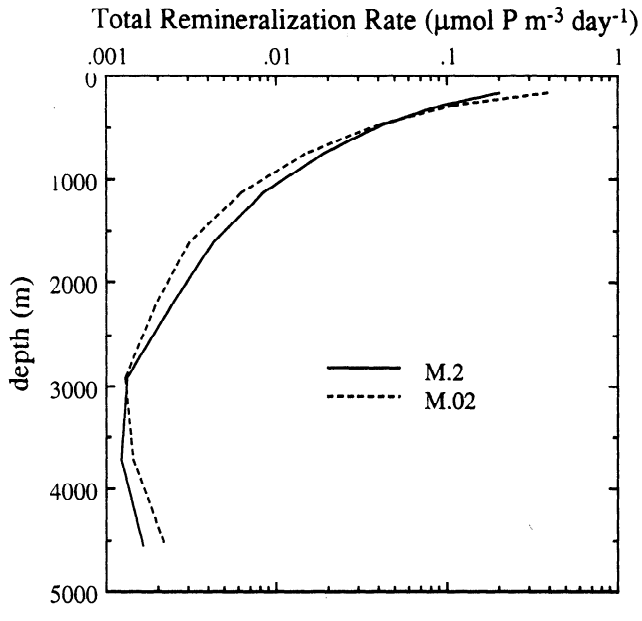

Figure 9. Total remineralization rates versus depth for models M.2 and M.02.

tations of the physical model. They avoid the problem of nutrient trapping often associated with particle-only models, even though only a small amount of DOP is used in M.02. Global mean new production in both models is within the range of observation-based estimates. DOP gradients across the base of the euphotic zone are greater than observed; these result from the requirement to export the large amount of DOP that is produced. Future work must involve allowing DOP to remineralize in the euphotic zone and/or decreasing the fraction of new production that is put into DOP.

4. Oxygen Simulation Experiments

For a given phosphate simulation (M.2 or M.02), the only remaining parameter needing to be defined for an oxygen simulation is the $-O_2/P$ remineralization ratio R_{remin}. The choices for R_{remin} and the resultant oxygen simulations will be described in the following subsections.

As oxygen saturation is a sensitive function of temperature (e.g., at 35‰ salinity, oxygen saturation at 5° C is 308 μmol/kg, and at 9° C is 281 μmol/kg, a difference of 27 μmol/kg), the "warm thermocline problem" causes oxygen concentrations in the model thermocline to be approximately 27 μmol/kg lower than observed. Thus a better alternative is to examine AOU ("apparent oxygen utilization" = $O_2^{sat} - O_2$), which is a measure primarily of biologically utilized oxygen. Surface AOU values (Figure 10) are approximately constant with temperature except in equatorial waters and the coldest waters below about 1°C, which do not ventilate the main thermocline. Thus, preformed thermocline AOU should be insensitive to flaws in the surface boundary conditions and isopycnal outcropping. The AOU distribution may still be affected, however, by other flaws in the model circulation.

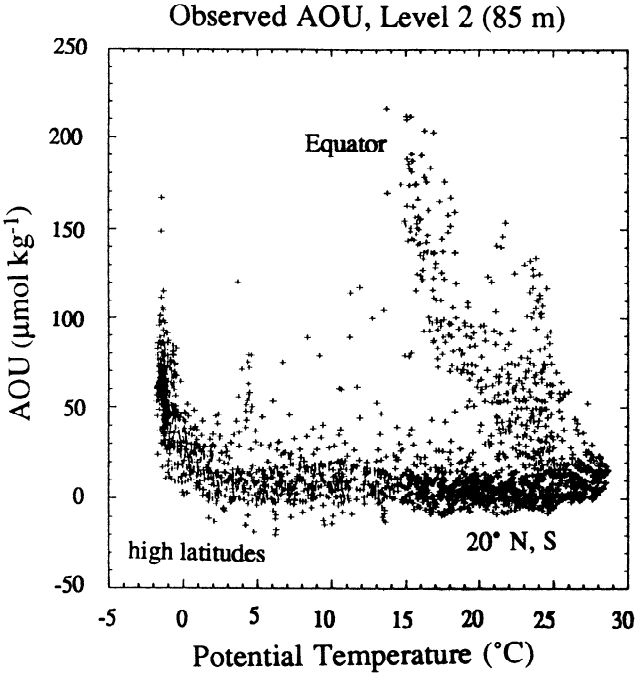

Figure 10. Observed AOU versus potential temperature on level 2 (85 m depth) in the world ocean. Waters with temperatures greater than 15° C are located between 20° N and 20° S, with highest AOU concentrations occurring at the equator.

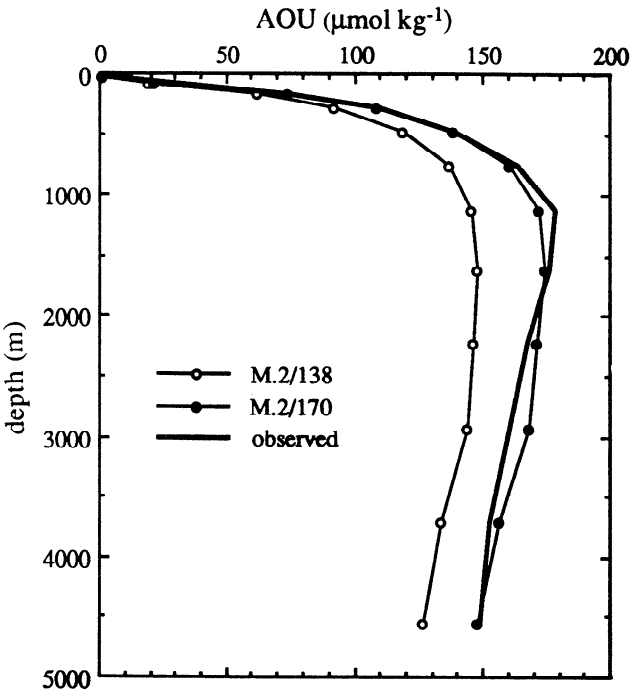

Figure 11. Global mean AOU versus depth, as observed and for models M.2/138 and M.2/170.

4.1. Deep Ocean Oxygen Simulations

Two oxygen simulations were run using the M.2 phosphate model, one with an $-O_2/P$ ratio of 138 matching that of *Najjar* [1990], and the other with a ratio of 170 matching more recent observational constraints. These simulations will be referred to as M.2/138 and M.2/170, respectively. These experiments were conducted to determine why previous oxygen simulations using an $-O_2/P$ ratio near 170 led to such poor results [*Najjar*, 1990]. The global AOU profiles for these simulations are shown in Figure 11. It can be seen that using an $-O_2/P$ ratio of 170 gives quite a good fit to observations, while a ratio of 138 results in an AOU profile that is much too low. Looking at each individual basin (Figure 12), we see that M.2/170 gives a better fit than M.2/138 in every basin, except the Atlantic. A scatter plot of AOU versus latitude on level 11 (Figure 13), however, shows that this offset is actually due to the absence of a low AOU northern end-member in the deep Atlantic, rather than too high an oxygen consumption (i.e., too high an $-O_2/P$ ratio); the AOU concentration of water entering the Atlantic from the Southern Ocean is actually more realistic in M.2/170 than in M.2/138.

The global mean AOU in the bottom box of the euphotic zone (level 2) for model M.2/170 is 21 μmol/kg, and in the Southern Ocean is 39 μmol/kg. These are similar to values used in previous box modeling work for high latitude "preformed" AOU (e.g., 30 μmol/kg used by *Toggweiler and Sarmiento*, 1985).

We now compare the M.2/170 simulation with one using the M.02 model and an $-O_2/P$ ratio of 170, which will be referred to as the M.02/170 simulation. The AOU profiles of M.02/170 and M.2/170 for the global ocean and the individual basins are shown in Figures 14 and 15, respectively. One can see that M.02/170 gives a worse fit than M.2/170 for the global mean and for every basin, except the Atlantic, in which both are comparable. These

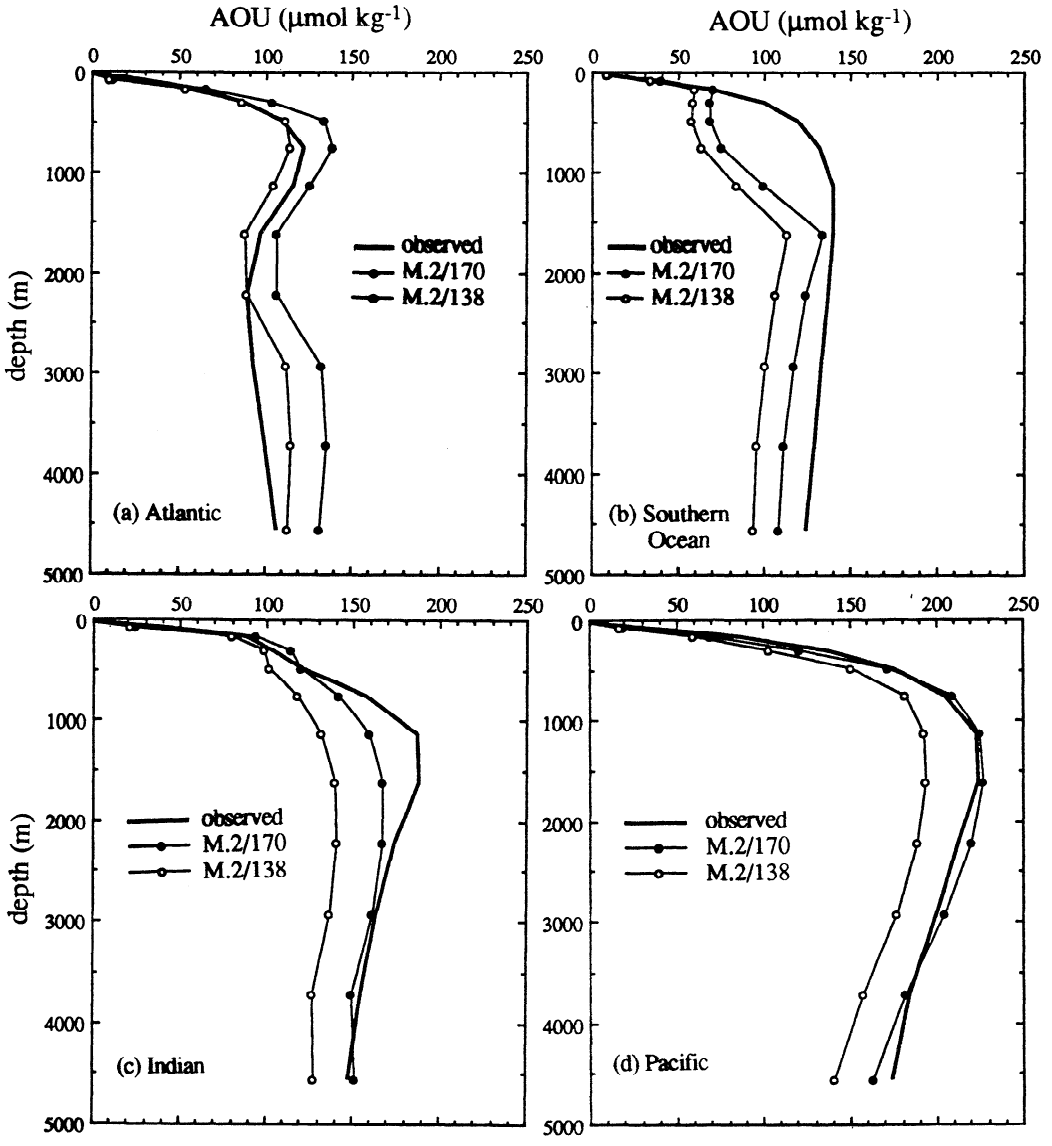

Figure 12. Basin mean AOU profiles, as observed and for models M.2/138 and M.2/170: (a) Atlantic, (b) Southern Ocean (defined as south of 48.9° S), (c) Indian, and (d) Pacific.

low M.02 AOU values at intermediate depths (evident particularly in the Indian and Pacific) are not due to preformed values, as surface AOU is low and similar in both models (Figure 15), and remineralization above 400 m (which may affect preformed AOU) is actually higher in M.02 than in M.2. Rather, it is due to the low remineralization rates at intermediate depths in M.02, shown in Figure 9. That is, this change in the shape of the AOU profile as $[DOP]_{avg}$ is decreased (from 0.2 in M.2/170 to 0.02 in M.02/170) is due to the fact that DOP in these models plays an important role in middepth remineralization rates. Note that changing the labile DOP concentration and hence the remineralization rate profile changes the vertical "shape" of the AOU profile (Figure 14), while changing the $-O_2/P$ ratio from 170 to 138 causes an offset in the AOU profile which is constant with depth below approximately 800 m (Figure 11).

The observed nutrient distributions indicate the deep ocean $-O_2/P$ remineralization ratio is near 170 [*Anderson and Sarmiento,* 1994]. Of the two models with an $-O_2/P$ ratio of 170, M.2/170 gives a better fit to the observed AOU and PO_4 profiles than M.02/170, suggesting that M.2/170 has a more realistic total remineralization profile. However, this does not mean necessarily that M.2/170 has the most realistic biological parameterization. Indeed, the average DOP concentration in M.2 is higher than observed by an order of magnitude.

One interpretation of the success of M.2/170 is that the addition of DOP, which deepens the total remineralization profile, may be compensating for an incorrect POP remineralization profile. That is, the open ocean composite POC remineralization profile of *Martin et al.* [1987] on which we base our model may be too shallow. There is some evidence to support this interpretation. For one thing, it appears that POM in highly productive regions undergoes deeper remineralization than POM in open ocean regions [*Knauer et al.,* 1979]. In addition, *Michaels et al.* [1990] have suggested that Martin et al.'s shallow traps overestimate the

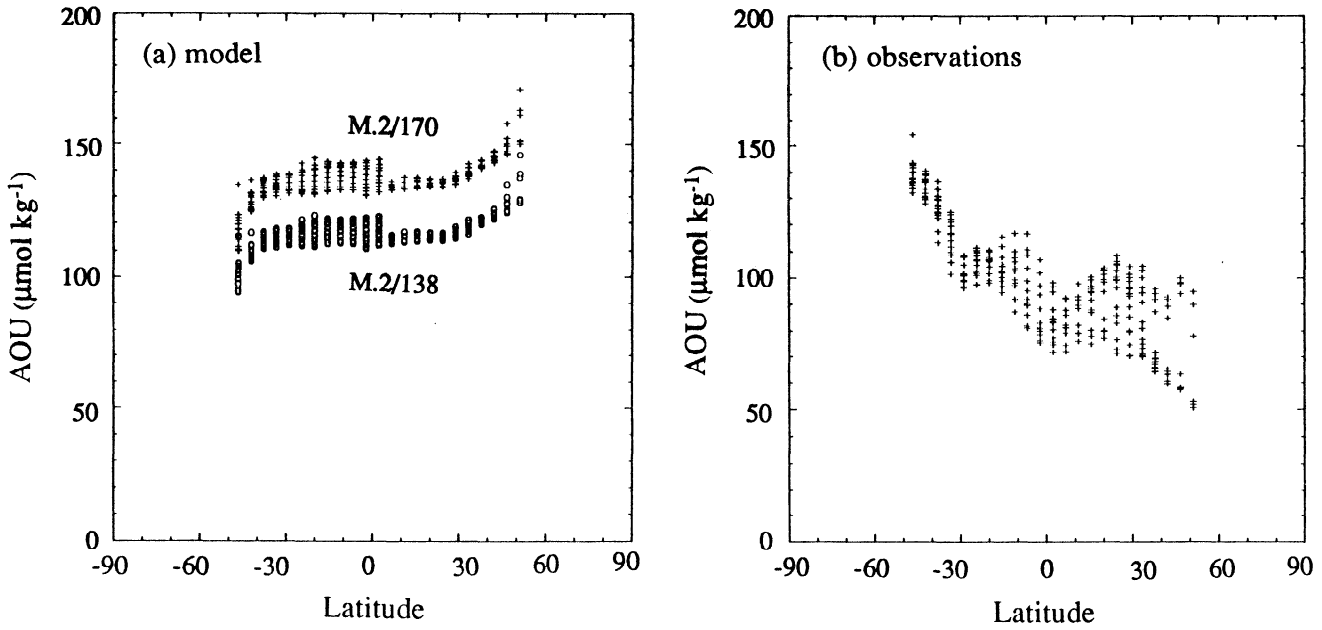

Figure 13. AOU versus latitude on level 11 (3721 m depth) in the Atlantic Ocean: (a) models M.2/170 and M.2/138, and (b) observations.

POM flux due to incomplete removal of swimmers. The POM flux profiles that Michaels et al. obtain, after correcting for this swimmer problem, imply deeper remineralization. Increasing the POP remineralization lengthscale might give a good fit similar to M.2/170 but without the need for such a high DOP concentration.

A second possible interpretation is that M.2/170 is successful because the 0.2 μmol/kg of DOP used in the model actually represents DOC and its impact on AOU. This implies that the actual remineralization of DOM may not follow Redfield stochiometry. One way to verify this interpretation is to model the non-Redfieldian DOC explicitly; such simulations are currently being carried out.

A third possible interpretation for the finding that the high DOP simulation M.2/170 does better than the simulation with a more realistic DOP of 0.02 μmol/kg is that the remineralization profile is compensating for flaws in the physical circulation. There are two main ways in which a flawed circulation can effect the nutrient distributions, (a) through giving incorrect preformed values, and (b) by a sluggish circulation (i.e., a low ventilation rate) enhancing the impact of the remineralization rate (or the converse). We have already shown that the first of these is a problem for the PO_4 distribution, but we have also already corrected for the effect of this. The impact of preformed values on the deep AOU distribution is negligible. The ocean circulation model definitely has problems in the deep North Atlantic, and also in the formation of proper intermediate water, but radiocarbon simulations show the ventilation rates to be generally reasonable otherwise [*Toggweiler et al.* 1989a,b]. It is difficult to see how the circulation could be modified in a manner consistent with the radiocarbon observations that would also give a more realistic simulation with the lower DOP concentration of 0.02 μmol/kg.

Najjar [1990] drew the conclusion that 138 was a more accurate $-O_2/P$ ratio than 170 because his 138 simulation fit the observed AOU distribution better at middepths, even though 172 gave a better fit in the deep ocean. In actuality, his model ED4 had been "tuned" to give a close fit to PO_4 observations, compensating for the warm thermocline deficiency in the physical model by using a large amount of DOP. This shifted more remineralization into intermediate depths and, as a result of PO_4 conservation, decreased the deep ocean PO_4 values. This is why AOU was too high in intermediate depths for a good deep ocean fit (namely, the 172 scenario), and too low in the deep ocean for a good intermediate depth fit (the 138 scenario). By decreasing the importance of DOM in the model (as done here in M.2), the remineralization rates at intermediate depths are much lower, such that a good fit in both intermediate depths and the deep ocean is obtained with an $-O_2/P$ ratio of 170.

What about the conclusions of the ocean general circulation model (OGCM) study by *Bacastow and Maier-Reimer* [1990] supporting a lower $-O_2/P$ ratio? Although *Bacastow and Maier-Reimer* [1990] get low O_2 concentrations when using an $-O_2/P$ ratio of 135, and therefore comment that a ratio of 177 would yield even worse results, their PO_4 values are much too high at the same depths that O_2 is low (especially beneath equatorial regions), suggesting that there is a problem with their remineralization length scale; namely, that their middepth remineralization rates are too high. They also admit that the low deep ocean O_2 values may be a consequence of weak NADW ventilation, a failing of the physical model [*Bacastow and Maier-Reimer,* 1990, p. 113]. More recently and in contrast with this earlier study, *Maier-Reimer* [1993] has obtained realistic nutrient distributions using an $-O_2/P$ of 177.

In conclusion, by decreasing the role of DOP in the model, which had been inappropriately used to compensate for flaws in the physical model, realistic PO_4 and AOU distributions can be obtained which are consistent with a deep ocean $-O_2/P$ ratio of 170.

4.2. Sensitivity to the Upper Ocean $-O_2/P$ Ratio

A last oxygen simulation was used to test the sensitivity of the O_2 simulation to the $-O_2/P$ ratio above 400 m, a region where the

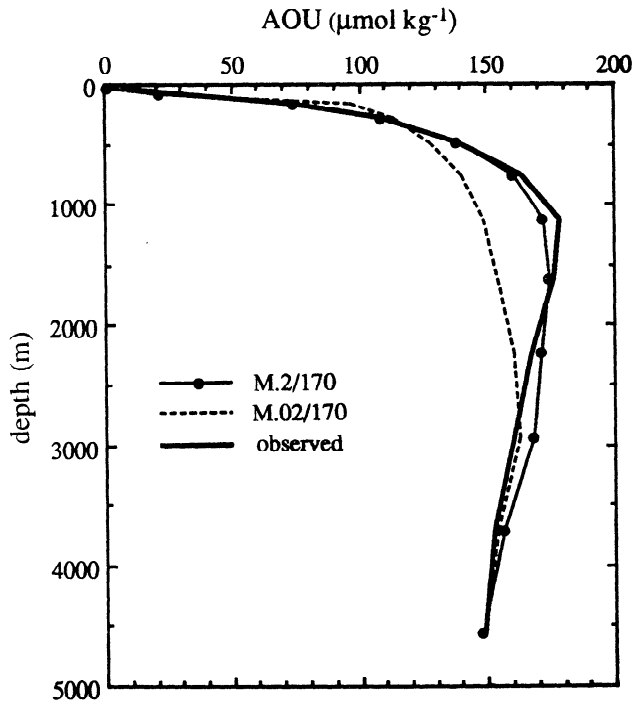

Figure 14. Global mean AOU versus depth, as observed and for models M.2/170 and M.02/170.

oxygen-to-phosphate stoichiometric ratios are poorly known. Our concern is that the upper ocean ratios might affect the deep ocean O_2 distribution and therefore the conclusions of the preceding section. It was surmised that the global O_2 distribution might be particularly sensitive to the upper ocean $-O_2/P$ ratio in high latitudes, if it affects preformed O_2 concentrations of deep water (through strong remineralization just beneath these regions of high new production).

In this simulation, called M.2/138-70, the $-O_2/P$ remineralization ratio (R_{remin}) was chosen to increase from a value of 138 at level 3 (just below the euphotic zone) to a value of 170 at depth by means of an exponential function, $R_{remin} = 170 - 32 \exp(-.005 (z - z_3))$, where z is the level depth (positive, in meters) and z_3 is the depth of level 3 (169.5 m). This function, illustrated in Figure 16, reaches a value of approximately 165 at 500 m, the depth by which, from the analyses of *Takahashi et al.* [1985] and *Anderson and Sarmiento* [1994], it is known that the $-O_2/P$ ratio is close to 170. The oxygen-to-phosphorus ratio in the euphotic zone (R_{photo}) was determined in the same way as in the previous simulations, by balancing O_2 consumption with O_2 production.

The global mean AOU profile for the M.2/138-70 simulation is shown in Figure 17a, along with those given by M.2/170 and M.2/138 for comparison. As can be seen, below 500 m the M.2/138-70 simulation is basically identical with that of M.2/170; this is true for every basin (not shown). While the lower $-O_2/P$ remineralization ratios on level 3 do cause AOU concentrations there to be 8 μmol/kg lower (Figure 17b), this offset does not translate into the deep ocean. In fact, in the Southern Ocean (not shown), the AOU offset on level 3 is only 4 μmol/kg. Apparently, the deep ocean AOU distribution is rather insensitive to the upper ocean $-O_2/P$ ratios, within the range of reasonable utilization ratio values (i.e., the offset would most likely still be negligible for upper ocean stoichiometric ratios as low as 100, or as high as 240).

This finding that deep AOU concentrations are not sensitive to $-O_2/P$ remineralization ratios (i.e., rates) above 500 m is surprising, as the magnitude of production and remineralization is generally high in high latitudes where preformed nutrient concentrations for the deep ocean are determined. Assuming a new production of 10 mol C m^{-2} yr^{-1} as typical of formation regions (Figure 7), an $-O_2/C$ ratio of 1.4 [*Anderson*, 1995], and that 75% of this new production remineralizes above 500 m [*Martin et al.*, 1987], we obtain an average remineralization rate of 26 μmol O_2 kg^{-1} yr^{-1} in the 100 to 500 m zone. The small impact of this shallow remineralization on deep AOU concentrations is probably a consequence of the short residence time of water in deep water formation regions. Convection, which is parameterized in the model as vertical homogenization of layers that are gravitationally unstable, is active over 75% of the time in these regions [*Toggweiler et al.*, 1989a]. Even if the residence time of water were as long as a month, the impact of upper thermocline remineralization would be reduced to 2 μmol kg^{-1} of O_2.

In the real ocean, one would expect the coupling between upper ocean remineralization rates and deep ocean AOU to be even weaker than in the model. Deep waters form in high latitudes in the winter season when production is presumably low due to low incident light and deep mixing. In addition, the sinking of cooled water to the deep ocean can be quite rapid.

As expected, the M.2/138-70 O_2 simulation approaches that of M.2/138 rather than M.2/170 above 500 m (Figure 17b). However, as M.2/170 actually gives a better fit to observations here, this is not seen as an advantage.

The value of R_{remin} above 500 m has an important impact upon the global denitrification rate. The amount of water column denitrification in M.2/138-70 (189 Tg N yr^{-1}, calculated as two thirds the O_2 consumption that "would have occurred" in anoxic regions) is closer to values estimated from observations (60-80 Tg N yr^{-1} [*Devol*, 1991]) than that of M.2/170 (306 Tg N yr^{-1}). The lower $-O_2/P$ ratios in M.2/138-170 reduce the size of anoxic zones above 500 m, and therefore the denitrification rate. However, as the physical model's "warm thermocline problem" results in lower-than-observed middepth oxygen concentrations, an accurate biological model should cause larger anoxic zones and a higher denitrification rate than observed. Without an improved thermocline circulation, it is difficult to infer the success of a biological model based upon its denitrification rate.

5. Discussion

We found that the misfits of the phosphate simulations to observations are primarily due to shortcomings of the physical model, rather than the biological model. We did not "tune" the biological model to give a better fit to phosphate observations, as this would have caused the biological cycle to become unrealistic in compensating for the physical model, which would have undesirable effects on the other nutrient simulations (i.e., O_2 and CO_2).

It should also be recognized that, due to the large number of necessary parameterizations in this model, the uncertainties in these parameterizations, and the sensitivity of the results to these uncertainties, such an OGCM cannot be effectively used to determine the deep ocean $-O_2/P$ ratio. The same may be said of box

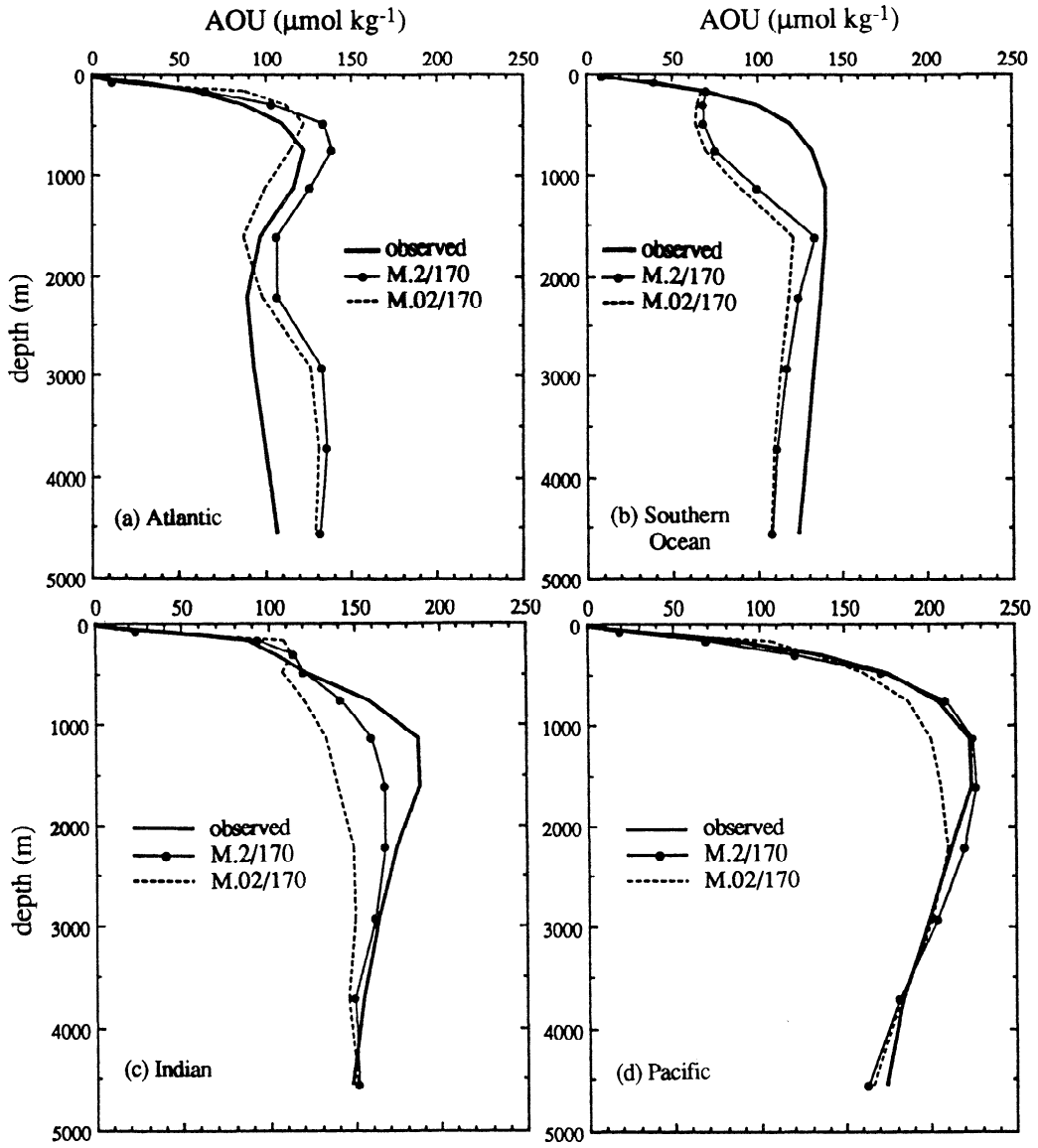

Figure 15. Basin mean AOU profiles, as observed and for models M.2/170 and M.02/170: (a) Atlantic, (b) Southern Ocean (defined as south of 48.9° S), (c) Indian, and (d) Pacific.

models. For example, consider the three-box model of *Sarmiento and Toggweiler* [1984], which is pictured in Figure 18. Balancing the budget of the deep-ocean box yields the following equations for phosphate and oxygen, respectively:

$$P_l + P_h = (T + f_{hd})(PO_{4d} - PO_{4h})$$

$$-R\,(P_l + P_h) = (T + f_{hd})(O_{2d} - O_{2h})$$

Combining these equations yields

$$R = (O_{2h} - O_{2d})(PO_{4d} - PO_{4h})$$

where the subscript d stands for concentrations in the deep ocean box, h stands for concentrations in the high-latitude box, and R is the $-O_2/P$ ratio. If we use the values suggested by *Sarmiento* [1986] for the observed nutrient concentrations in these boxes, we find

$$R = (340 - 166)/(2.1 - 1.1) = 174$$

consistent with the results of section 4. However, using slightly different values (within the range of uncertainty, given the arbitrariness of the "boxes" as summaries of oceanographic regions, and the uncertainty in high-latitude preformed concentrations that influence deep ocean properties) can give a much lower ratio:

$$R = (330 - 170)/(2.2 - 1.0) = 134$$

Thus the $-O_2/P$ ratio estimates are too sensitive to the physical and biological uncertainties and parameterizations in both box models and OGCMs to be determined to an accuracy better than by other methods. The essential proof for stoichiometric ratios must come from the more direct analysis of nutrient data [e.g., *Takahashi et al.*, 1985; *Anderson and Sarmiento*, 1994]. The role

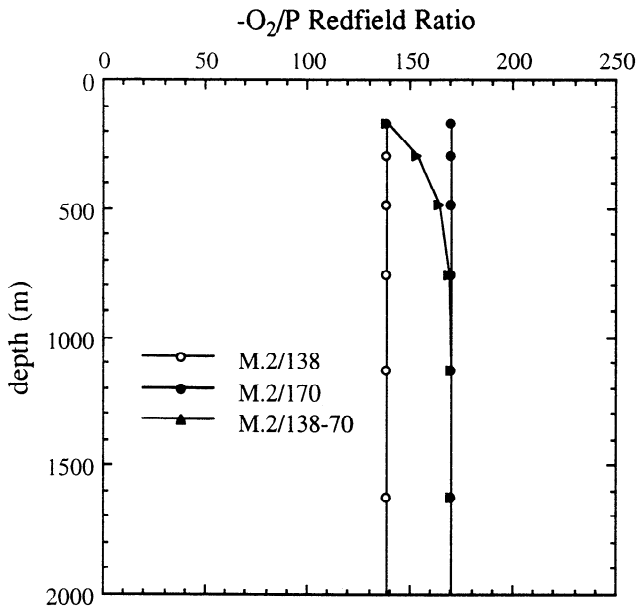

Figure 16. The $-O_2/P$ ratio versus depth as used in models M.2/138, M.2/170, and M.2/138-70.

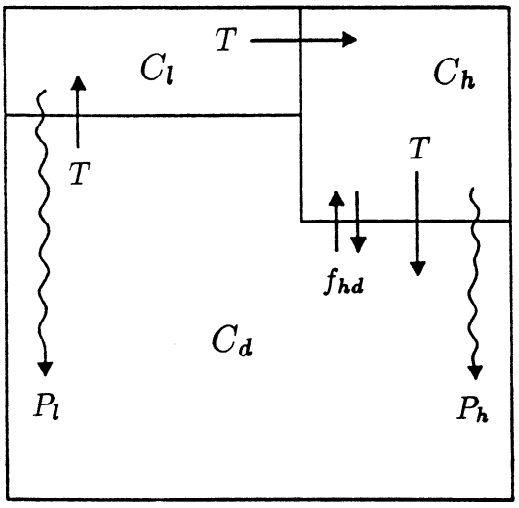

Figure 18. Three-box ocean model of *Sarmiento and Toggweiler* [1984]. C stands for a nutrient concentration (moles per cubic meter), T for the thermohaline watermass transport (cubic meters per second), f for convective mixing (cubic meters per second), and P for organic particle flux (moles per second). Subscripts h, l and d denote properties relating to the high-latitude surface, low-latitude surface, and deep ocean model boxes, respectively. The balance of the deep ocean box yields the equation $P_l + P_h = (T + f_{hd})(C_d - C_h)$.

of modeling studies is to find out how this information fits into a synthesized understanding of ocean nutrient cycling, and what the possible implications are for the less well understood processes.

A conclusion can be drawn, however, regarding the combined vertical remineralization profile from dissolved and particulate organic matter, which is less well known. Previous estimates include those calculated from sediment trap fluxes [*Martin et al.*, 1987], ETS activity [*Packard et al.*, 1988], and ^{3}He data [*Jenkins*, 1982], but such measurements are sparse in space and time, such that their relation to global mean rates is unclear. The above simulations illustrate that the AOU distribution is a sensitive indicator of remineralization rates. As the M.2/170 simulation gives a good fit to both global mean observed AOU and PO_4 (within con-

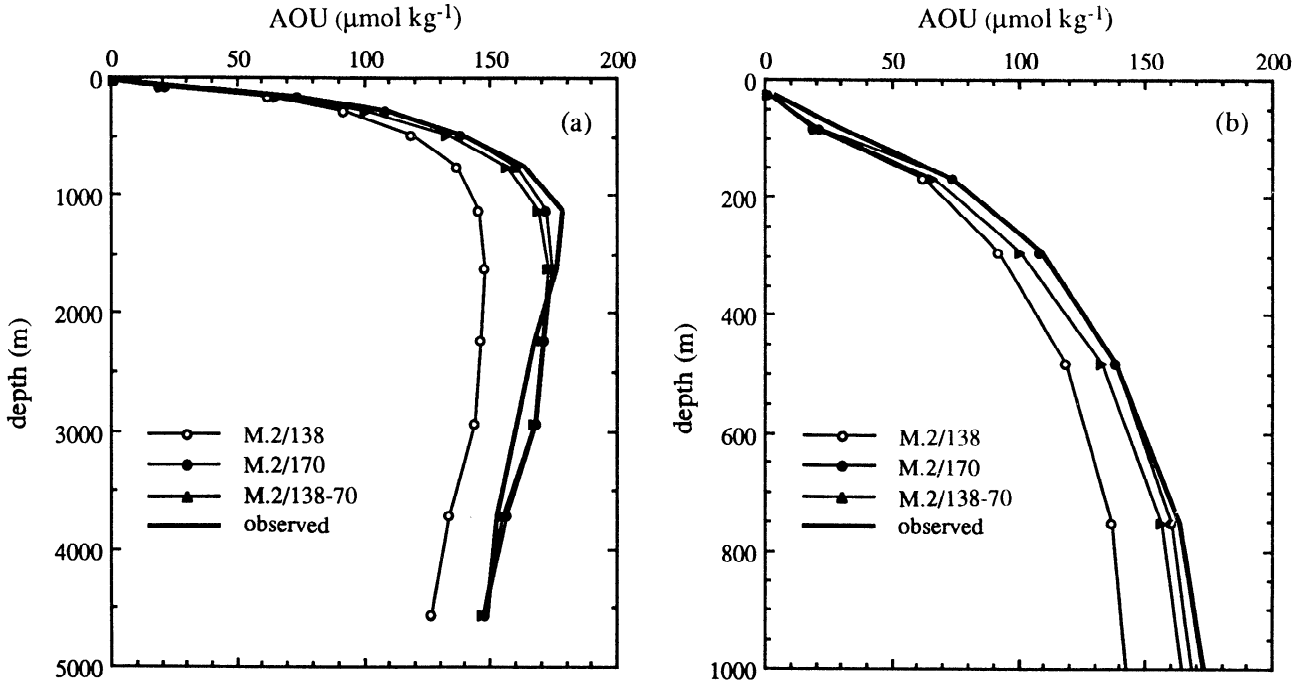

Figure 17. Global mean AOU versus depth, for models M.2/138, M.2/170, and M.2/138-70: (a) the entire water column, and (b) the upper 1000 m.

text of the circulation), the M.2 total remineralization profile may be fairly realistic. The accuracy of the total remineralization rate, however, relies on the accuracy of the physical model's rate of ventilation. The DOP simulation has faults, and it is possible that the division between DOM and POM remineralization is not correctly represented. Clarification on this topic awaits further direct observations, and further modeling investigation. However, whatever the role of DOM, it appears that the total remineralization rate profile has a somewhat deeper lengthscale than has been suggested by the sediment trap fluxes of *Martin et al.* [1987].

A final recognition this study brings out is the usefulness of AOU in validating biological model parameterizations. Because preformed AOU values are low and similar over most of the surface ocean, AOU in a model is not as strongly affected by model circulation problems as other nutrients. For the same reason, deep ocean AOU is also almost completely the result of biological utilization, and as such the AOU distribution should give a better indication of the accuracy of the remineralization distribution than other nutrients. Given the strong evidence that the $-O_2/P$ ratio below 400 m is near 170, and the insensitivity of deep ocean AOU to surface ocean $-O_2/P$ ratios, it seems AOU may be used with relative confidence in verifying the accuracy of biological parameterizations at depth in model simulations.

Acknowledgments. Many thanks to R. Toggweiler, R. Najjar, J. Orr, and R. Murnane for instruction and comments during the course of this study. Thanks also to the reviewers, amongst whom were M. Bender and E. Maier-Reimer, whose comments helped redirect the paper's emphasis. This work was supported by the Joint Global Ocean Flux Study of the National Science Foundation (OCE 90-12333) as well as the U. S. Department of Energy under contract DEFG 02-90ER61052, and GFDL/NOAA through the generosity of K. Bryan and J. Mahlman.

References

Anderson, L. A., On the hydrogen and oxygen content of marine phytoplankton, *Deep Sea Res.*, in press, 1995.

Anderson, L. A., and J. L. Sarmiento, Redfield ratios of remineralization determined by nutrient data analysis, *Global Biogeochem. Cycles*, *8*, 65-80, 1994.

Bacastow, R., and E. Maier-Reimer, Ocean-circulation model of the carbon cycle, *Clim. Dyn.*, *4*, 95-125, 1990.

Bacastow, R., and E. Maier-Reimer, Dissolved organic carbon in modeling oceanic new production, *Global Biogeochem. Cycles*, *5*, 71-85, 1991.

Bainbridge, A. E. (Ed.), *GEOSECS Atlantic Expedition, Vol. 2, Sections and Profiles*, 198 pp., U. S. Govt. Print. Off., Washington, D. C., 1981.

Benner, R., J. D. Pakulski, M. McCarthy, J. I. Hedges, and P. G. Hatcher, Bulk chemical characteristics of dissolved organic matter in the ocean, *Science*, *255*, 1561-1564, 1992.

Broecker, W. S., T. Takahashi, and T. Takahashi, Sources and flow patterns of deep-ocean waters as deduced from potential temperature, salinity, and initial phosphate concentration, *J. Geophys. Res.*, *90*, 6925-6939, 1985.

Cho, B. C., and F. Azam, Major role of bacteria in biogeochemical fluxes in the ocean's interior, *Nature*, *332*, 441-443, 1988.

Devol, A. H., Direct measurement of nitrogen gas fluxes from continental shelf sediments, *Nature*, *349*, 319-321, 1991.

Eppley, R. W., New production: History, methods, problems, in *Productivity of the Ocean: Present and Past*, edited by W. H. Berger et al., pp. 85-97, John Wiley, New York, 1989.

Esbensen, S. K., and Y. Kushnir, The heat budget of the global ocean: An atlas based on estimates from surface marine observations, *Rep. 29*, Clim. Res. Inst., Oreg. State Univ., Corvallis, 1981.

Hellerman, S., and M. Rosenstein, Normal monthly wind stress over the world ocean with error estimates, *J. Phys. Oceanogr.*, *13*, 1093-1104, 1983.

Jackson, G. A., and P. M. Williams, Importance of dissolved organic nitrogen and phosphorus to biological nutrient cycling, *Deep Sea Res. Part A*, *32*, 223-235, 1985.

Jenkins, W. J., Oxygen utilization rates in North Atlantic subtropical gyre and primary production in oligotrophic systems, *Nature*, *300*, 246-248, 1982.

Keeling, R. F., and S. R. Shertz, Seasonal and interannual variations in atmospheric oxygen and implications for the global carbon cycle, *Nature*, *358*, 723-727, 1992.

Knauer, G. A., J. H. Martin and K. W. Bruland, Fluxes of particulate carbon, nitrogen, and phosphorus in the upper water column of the northeast Pacific, *Deep Sea Res. Part A*, *26*, 97-108, 1979.

Levitus, S., Climatological atlas of the world ocean, *NOAA Prof. Pap. 13*, 1982.

Levitus, S., M. E. Conkright, J. L. Reid, R. G. Najjar and A. Mantyla, Distribution of nitrate, phosphate and silicate in the world oceans, *Prog. Oceanogr.*, *31*, 245-273, 1993.

Liss, P. S., and L. Merlivat, Air-sea gas exchange rates: Introduction and synthesis, in *The Role of Air-Sea Exchange in Geochemical Cycling*, edited by P. Buat-Menard, NATO ASI Series, series C, *185*, pp. 113-127, D. Reidel, Norwell, Mass., 1986.

Maier-Reimer, E., Geochemical cycles in an ocean general circulation model. Preindustrial tracer distributions, *Global Biogeochem. Cycles*, *7*, 645-677, 1993.

Martin, J. H., G. A. Knauer, D. M. Karl and W. W. Broenkow, VERTEX: Carbon cycling in the northeast Pacific, *Deep Sea Res. Part A*, *34*, 267-285, 1987.

Michaels, A. F., M. W. Silver, M. M. Gowing, and G. A. Knauer, Cryptic zooplankton "swimmers" in upper ocean sediment traps, *Deep Sea Res. Part A*, *37*, 1285-1296, 1990.

Murray, J. W., R. T. Barber, M. R. Roman, M. P. Bacon, and R. A. Feely, Physical and biological controls on carbon cycling in the Equatorial Pacific, *Science*, *266*, 58-65, 1994.

Najjar, R. G., Simulations of the phosphorus and oxygen cycles in the world ocean using a general circulational model, Ph.D. thesis, 190 pp., Princeton Univ., Princeton, N. J., 1990.

Najjar, R. G., J. L. Sarmiento, and J. R. Toggweiler, Downward transport and fate of organic matter in the ocean: Simulations with a general circulation model, *Global Biogeochem. Cycles*, *6*, 45-76, 1992.

Packard, T. T., M. Denis, M. Rodier, and P. Garfield, Deep-ocean metabolic CO_2 production: Calculations from ETS activity, *Deep Sea Res.*, *35*, 371-382, 1988.

Redfield, A. C., B. H. Ketchum, and F. A. Richards, The influence of organisms on the composition of sea-water, in *The Sea*, vol. 2, edited by M. N. Hill, pp. 26-77, Wiley-Interscience, New York, 1963.

Ridal, J. J., and R. M. Moore, A re-examination of the measurement of dissolved organic phosphorus in seawater, *Mar. Chem.*, *29*, 19-31, 1990.

Sambrotto, R. N., G. Savidge, C. Robinson, P. Boyd, T. Takahashi, D. M. Karl, C. Langdon, D. Chipman, J. Marra, and L. Codispoti, Elevated consumption of carbon relative to nitrogen in the surface ocean, *Nature*, *363*, 248-250, 1993.

Sarmiento, J. L., Modeling oceanic transport of dissolved constituents, in *The Role of Air-Sea Exchange in Geochemical Cycling*, edited by P. Buat-Menard, NATO ASI Series, series C, *185*, pp. 65-82, D. Reidel, Norwell, Mass., 1986.

Sarmiento, J. L., and J. R. Toggweiler, A new model for the role of the oceans in determining atmospheric pCO_2, *Nature*, *308*, 621-624, 1984.

Sugimura, Y., and Y. Suzuki, A high-temperature catalytic oxidation method for the determination of non-volatile dissolved organic carbon in seawater by direct injection of a liquid sample, *Mar. Chem.*, *24*, 105-131, 1988.

Suzuki, Y., On the measurement of DOC and DON in seawater, *Mar. Chem.*, *41*, 287-288, 1993.

Suzuki, Y., Y. Sugimura, and T. Itoh, A catalytic oxidation method for the determination of total nitrogen dissolved in seawater, *Mar. Chem.*, *16*, 83-97, 1985.

Takahashi, T., W. S. Broecker, and S. Langer, Redfield ratio based on chemical data from isopycnal surfaces, *J. Geophys. Res.*, *90*, 6907-6924, 1985.

Toggweiler, J. R., K. Dixon, and K. Bryan, Simulations of radiocarbon in a coarse-resolution world ocean model, 1, Steady state prebomb distributions, *J. Geophys. Res.*, *94*, 8217-8242, 1989a.

Toggweiler, J. R., K. Dixon, and K. Bryan, Simulations of radiocarbon in

a coarse-resolution world ocean model, 2, Distributions of bomb-produced ^{14}C, *J. Geophys. Res., 94*, 8243-8264, 1989b.

Toggweiler, J. R, and J. L Sarmiento, Glacial to interglacial changes in atmospheric carbon dioxide: The critical role of ocean surface water in high latitudes, in *The Carbon Cycle and Atmospheric CO_2: Natural Variations Archean to Present*, Geophys. Monogr. Ser., vol. *32*, edited by E. T. Sundquist and W. S. Broecker, pp. 163-184, AGU, Washington, D. C., 1985.

Walsh, J., A data set on northern hemisphere sea ice extent, 1953-1976, *Glacialogical Data, Rep. GD-2*, 49-51, World Data Cent. for Glaciol. (Snow and Ice), Boulder, Colo., 1978.

Walsh, T. W., Total dissolved nitrogen in seawater: A new high-temperature combustion method and a comparison with photo-oxidation, *Mar. Chem., 26*, 295-311, 1989.

Wanninkhof, R., Relationship between wind speed and gas exchange over the ocean, *J. Geophys. Res., 97*, 7373-7382, 1992.

Weiss, R. F., The solubility of nitrogen, oxygen and argon in water and seawater, *Deep Sea Res., 17*, 721-735, 1970.

You, Y., and M. Tomczak, Thermocline circulation and ventilation in the Indian Ocean derived from water mass analysis, *Deep Sea Res. Part I, 40*, 13-56, 1993.

Zwally, H. J., J. Comiso, C. Parkinson, W. Campbell, F. Carsey, and P. Gloerson, *Antarctic Sea Ice, 1973-1976: Satellite Passive-Microwave Observations*, 206 pp., Natl. Aeron. Space Admin., Washington, D. C., 1983.

L. Anderson, Division of Applied Sciences, Harvard University, 29 Oxford St., Cambridge, MA 02138. (e-mail: larrya@pacific.harvard.edu)

J. L. Sarmiento, Progam in Atmospheric and Oceanic Sciences, Sayre Hall, Forrestal Campus, Princeton University, Princeton, NJ 08544. (e-mail: jls@splash.princeton.edu)

(Received January 12, 1994; revised June 12, 1995; accepted June 20, 1995.)